Available online at www.sciencedirect.com
SCIENCE DIRECT®
Polymer 45 (2004) 1939–1950
polymer
www.elsevier.com/locate/polymer

Controlled degradation of epoxy networks: analysis of crosslink density and glass transition temperature changes in thermally reworkable thermosets

Jir-Shyr Chen[a], Christopher K. Ober[a,*], Mark D. Poliks[b], Yuanming Zhang[a], Ulrich Wiesner[a], Claude Cohen[c]

[a]*Department of Materials Science and Engineering, Cornell University, 310 Bard Hall, Ithaca, NY 14853, USA*
[b]*Endicott Interconnect Technologies, Endicott, NY 13760, USA*
[c]*School of Chemical Engineering, Cornell University, Ithaca, NY 14853, USA*

Received 2 January 2004; accepted 9 January 2004

Abstract

The characteristics of networks formed in cured 'reworkable' epoxy thermosets capable of controlled thermal degradation were studied. Dynamic mechanical thermal analysis, swelling measurements, and glass transition temperature measurements were used to obtain information regarding the time and temperature dependence of the crosslink densities of these materials. By applying isothermal conditions, networks containing up to 36 mol% non-degradable components could be completely degraded, i.e. progress from a network of infinite molecular weight to a finite one with zero crosslink density. Percolation theory was used to facilitate the interpretation of these results. The degradation behavior of the reworkable thermosets were well-described by gel degradation theory, i.e. the reverse of the gelation process, and the experimental results were in good agreement with calculated values obtained by replacing the extent of reaction, p, in Macosko and Miller's branching theory with the extent of degradation, $1 - p$.

Keywords: Network degradation; Reworkable thermoset; Crosslink density

1. Introduction

Epoxy resins were first introduced to the world in 1946 at the Swiss Industries Fair [1]. Since that time, epoxy compounds have found uses in a wide variety of applications, such as adhesives, surface coatings, and microelectronic encapsulants [2,3]. The importance of these materials and their widespread use today is due in large part to their excellent adhesive and thermal-mechanical properties, as well as their ease of processing. Once fully cured, epoxies form highly crosslinked, three-dimensional networks. The densely crosslinked nature of the material is what enables many of its superior properties. It is therefore no surprise that the mechanical properties of an epoxy are often linked directly to its crosslink density. As such, changes in crosslink density invariably lead to changes in ultimate properties.

In recent years, the microelectronics industry has developed a need for a class of materials known as 'reworkable' thermosets [4]. For a material to be successfully reworkable, it must have properties similar to or exceeding those of conventional thermoset materials, but must also be removable under controlled conditions. With conventional epoxy thermosets, the adhesive bond created between two attached components is usually permanent. The stable network structure of a typical epoxy resin means that neither solvent nor heat can be used to easily remove these materials. Several groups have created reworkable materials by employing various strategies including incorporating thermally or chemically cleavable groups into epoxy monomers [5–9]. However, regardless of the method chosen to enable reworkability, a key aspect common to all systems is that the crosslinked network must break apart when desired. In other words, the crosslink density of the

* Corresponding author. Tel.: +1-607-255-8417; fax: +1-607-255-6575.
E-mail address: cober@ccmr.cornell.edu (C.K. Ober).

0032-3861/$ - see front matter © 2004 Elsevier Ltd. All rights reserved.
doi:10.1016/j.polymer.2004.01.011

materials must be significantly reduced in a controlled manner to facilitate removal of the epoxy system [10].

As with conventional epoxy systems, much can be learned about a reworkable epoxy system by studying its crosslink density. Several methods are available for measuring the crosslink density of a thermoset, including the use of mechanical, swelling, and T_g measurements [11,12]. The most common method is to measure the elastic modulus of the thermoset in its rubbery regime (i.e. $T \gg T_g$) using a thermal mechanical testing instrument and then to apply theory to calculate the crosslink density. In applying the theory to epoxy materials, the primary assumption is that at temperatures much higher than the glass transition temperature, the epoxy thermosets exhibit rubbery behavior [13]. The use of swelling measurements to obtain quantitative crosslink density values of epoxy thermosets has been used with limited success [14,15]. However, swelling results do correlate well qualitatively to crosslink density measurements obtained via other routes. A third technique is to correlate the glass transition temperature of the material with its crosslink density [16]. Most expressions for doing so were derived empirically, but a few have some theoretical basis [17]. Generally, the use of thermal mechanical testing methods is considered the most accurate method for obtaining quantitative crosslink density values.

The objective of this work is to detail and understand the network characteristics of reworkable thermosets as they relate to crosslink densities and glass transition temperatures. In a previous paper, we discussed the degradation chemistry and kinetics of a thermally reworkable epoxy thermoset [10]. The epoxy monomer studied (α-Terp) was a cycloaliphatic diepoxide linked by a thermally cleavable tertiary ester linkage. When incorporated into a fully crosslinked network, the tertiary ester linkages enable reworkability of the thermoset by cleaving under selected thermal conditions, also called rework conditions. By examining the changes in T_g of the reworkable thermoset as a function of its rework conditions, it was found that T_g would decrease with time following an exponential-decay. This was attributed to a kinetically controlled reduction in the network crosslink density. However, a detailed investigation of the crosslink density of the thermoset was not conducted. Because the extent of network degradation can be controlled in these materials, they offer a wide range of possible crosslink densities while simultaneously maintaining a consistent molecular architecture. Both dynamic mechanical thermal analysis (DMTA) and swelling measurements were conducted to determine the crosslink densities of these materials. The crosslink densities were analyzed with respect to their isothermal behavior and were compared to their glass transition temperatures as measured by dynamic scanning calorimetry (DSC). Percolation theory was used to gain further insight into the network properties of these unique thermosets. Finally, the experimental results were modeled and analyzed using gel degradation theory [18–20] and Macosko and Miller's branching theory [21,22].

2. Experimental

2.1. Materials

The chemical structures of most of the compounds used in this study are detailed in Fig. 1. The original synthesis of the α-Terp epoxy monomer (based on α-terpineol) has been published elsewhere. The α-Terp epoxy monomer used in this study was donated by Loctite Corporation and was used as received. Hexahydro-4-methylphthalic anhydride (HHMPA), ethylene glycol (EG), *N*,*N*-dimethylbenzylamine (BDMA), sodium bromide, and methanol were used as received from Aldrich. ERL-4221™ (ERL), a cycloaliphatic diepoxide monomer originally made by Union Carbide, was donated by IBM Corporation and used as received.

2.2. Curing conditions

The epoxy monomers were crosslinked using HHMPA as a curing agent, EG as an initiator, and BDMA as a catalyst. The order in which samples were mixed is as follows: the epoxy monomers were first thoroughly mixed, followed by the additions of the curing agent, initiator, and catalyst—in that order. The catalyst was added last to minimize the advancement of the uncured samples at room temperature. A molar ratio of epoxide groups to HHMPA of 1.00–0.87 was used for all systems. The amount of initiator and catalyst used was 1.5% of the total weight for each compound. The mixed samples were subsequently degassed for a few minutes under vacuum at room temperature to remove any trapped air bubbles. Samples that were not used immediately were stored at −40 °C for later use. To crosslink the samples, the mixtures were first poured into either Teflon or silicone-rubber molds, then pre-cured in an oven at 110 °C for 1 h, followed by a final cure at 140 °C for

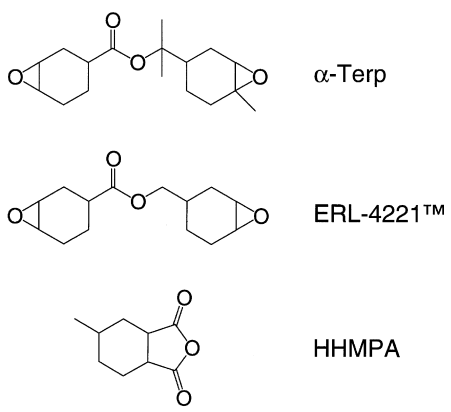

Fig. 1. Chemical structures of materials used. (α-Terp, alpha-terpineol based reworkable epoxy; ERP-4221™, cycloaliphatic epoxy; HHMPA, hexahydromethyl phthalic anhydride).

16 h. The samples were then allowed to cool to room temperature at a rate of approximately 1–2 °C/min.

2.3. Thermal degradation/rework conditions

The terminology 'rework condition' used in this paper refers to the amount of thermal treatment a fully-crosslinked epoxy sample received. The primary variables were the isothermal temperature and the length of time the system was kept at this temperature. All thermal treatments were conducted at 193 °C under an air atmosphere, unless otherwise noted. The exposure times ranged from 0-minutes, i.e. the as-cured material, to 640 min.

2.4. Sample matrix

For the swelling experiments, a set of reworkable materials were created by using varying amounts of α-Terp and ERL in the thermoset mixture, with the total mole ratio of epoxide groups to HHMPA constant at 1.0:0.87. The ERL component of the samples varied in increments of approximately 10 mol% with respect to the total amount of epoxy monomer. Each thermoset composition was cured then reworked under the prescribed conditions. The final sample matrix for the swelling experiments is shown in Table 1. Commercial silicone molds were used to create samples of uniform dimensions to allow for more consistent swelling measurements. Pieces were cut from each sample for DSC testing.

A similar set of α-Terp/ERL composite systems were created for DMTA measurements. After the systems were cured, they were machined to 20 mm × 5 mm × 1 mm pieces. These samples were not reworked prior to testing.

In referring to the epoxy mixtures used in this study, the naming convention AE-XX is used, where XX represents the percentage of α-Terp in the system. For example, a mixture containing 66% α-Terp and 34% ERL is referred to as AE-66.

2.5. Density measurements

Density measurements were conducted using a density gradient column kept at a constant 23 °C. A saturated solution of sodium bromide in distilled water was slowly mixed with distilled water to create a column with a density range of 1.100 g/ml to 1.300 g/ml. The column was calibrated using glass beads of known densities and was found to be linear across the given range ($R^2 > 0.994$). During measurements, care was taken to avoid air bubble formation on sample surfaces that may affect the density measurements. Based on repeated measurements, the estimated measurement errors were +/− 0.005 g/ml.

2.6. DMTA measurements and analysis

Samples were measured in torsional mode using a Rheometrics Scientific ARES rheometer to determine the shear modulus, G. For isothermal runs, a temperature ramp of 50 °C/min was used to reach the desired temperature, with a maximum overshoot of approximately +1.0 °C for under 1 min. All measurements were conducted at 1 Hz under a nitrogen atmosphere. The strain amplitude was kept constant at 0.4%.

From the statistical theory of rubber elasticity, the number of moles of crosslinked chains per unit volume, also known as the strand density, for an affine network is given by [23,24]

$$\nu = \frac{G}{RT} \tag{1}$$

where ν is the strand density, R is the universal gas constant, and T is the absolute temperature. Affine behavior is characterized by network chains and crosslinks that move proportionally to the macroscopic deformation of the system. This is in contrast to a phantom network where the crosslinks may fluctuate about their mean positions due to Brownian motion [12,25]. Also, for an ideal tetrafunctional network, the crosslink density is one-half the value of ν because there are two chains per crosslink site. Throughout the course of this report, the two terms, crosslink density and strand density, are both used, so a factor of two should be used to convert from one to the other. The molecular weight between crosslinks, M_C, is calculated by dividing the material's density by its strand density.

Table 1
Swelling sample composition matrix. Checkmarks (✓) represent samples that were successfully tested via swelling and × s represent samples that were not measured due to extensive degradation during swelling

Isothermal time @ 193 °C (min)	α-Terp (mole percent of total epoxy component)										
	0	10	19	27	36	46	55	66	77	88	100
0	✓	✓	✓	✓	✓	✓	✓	✓	✓	✓	✓
30	✓	✓	✓	✓	✓	✓	✓	✓	✓	✓	✓
61	✓	✓	✓	✓	✓	✓	✓	✓	✓	×	×
85	✓	✓	✓	✓	✓	✓	✓	✓	×	×	×
153	✓	✓	✓	✓	✓	✓	✓	✓	×	×	×
302	✓	✓	✓	✓	✓	✓	×	×	×	×	×
640	✓	✓	✓	✓	✓	✓	×	×	×	×	×

2.7. Swelling measurements and analysis

The samples were swollen in methanol for a total of 19 weeks. The swelling solvent was replaced with fresh solvent once a week and the used solvent containing extracted material was saved for later analyses. The samples were weighed periodically to gauge the extent of swelling. To prepare the samples for weighing, excess solvent on the surfaces of the samples was removed, and then the samples were placed into sealed vials to reduce solvent evaporation during the weighing. At the end of the swelling period, the samples were dried in a vacuum oven at 70 °C for 4 days and weighed again to determine m_d, the mass of the dry network after extraction of soluble materials.

To calculate the crosslink density of the swollen materials, the Flory–Rehner expression for a tetrafunctional affine network was used. The expression is given as [26–28]:

$$\nu = \frac{\ln(1-v_2) + v_2 + \chi v_2^2}{v_1\left(\frac{v_2}{2} - v_2^{\frac{1}{3}}\right)} \tag{2}$$

where ν is strand density, v_2 is the volume fraction of polymer at equilibrium swelling, χ is the polymer-solvent interaction parameter, and v_1 is the molar volume of the solvent. The polymer volume fraction is given by [29]

$$v_2 = \left[1 + \left(\frac{m_{eq} - m_d}{m_d}\right)\left(\frac{\rho_2}{\rho_1}\right)\right]^{-1} \tag{3}$$

where ρ_2 and ρ_1 are the densities of the polymer and solvent, respectively, and m_{eq} is the mass of the swollen network at equilibrium. As with the DMTA results, the strand density is twice the crosslink density for an ideal tetrafunctional network.

2.8. T_g measurements

Glass transition temperatures were measured using a TA Instruments DSC 910. All samples were placed in hermetically sealed aluminum DSC pans and heated at a rate of 20 °C/min under nitrogen. To determine T_g from the DSC data, the temperature at the computer-calculated transition midpoint was averaged with the temperature at which the maximum in the first-order derivative with respect to temperature was detected. The difference between the two measured values was typically on the order of a few degrees Celsius.

3. Results and discussions

3.1. Network characteristics

The chemical degradation mechanism and degradation kinetics of the reworkable thermoset used in this study have been described elsewhere [7,10]. However, a thorough discussion of the physical properties of these materials requires some background information on their chemical characteristics, thus a brief summary of those findings follows. It was found that cleavage of the tertiary ester linkages present in the α-Terp systems was consistent with known mechanisms established from ester degradation studies. At high temperatures, the tertiary ester groups cleave and form carboxylic acid groups and alkenes. Some of the carboxylic acid groups may further react to form acid anhydrides. The physical implication of such a degradation process is that each time an ester group is cleaved, the local crosslink density decreases. A proposed method to easily measure the change in the crosslink density of the system, and hence the reworkability of the system, is to measure the shift in the glass transition temperature of the networks as a function of the rework conditions. This method relies on the condition that the glass transition temperature varies in a systematic way with the crosslink density. By studying the T_g-shift, it was found that T_g varied with isothermal treatment time by the relationship

$$T_g = Ce^{-k_1 t} + De^{-k_2 t} + E \tag{4}$$

where C and D are pre-exponential factors, t is the time in minutes, k_1 and k_2 are rate constants, and E represents the glass transition temperature of the material with zero crosslinks.

3.1.1. Sample matrix

Many prior studies relating crosslink density changes to physical properties examined systems with varying crosslink densities made by changing the curing conditions and/or changing the molecular weights of the starting components [14,15,30–35]. The material set used for this study instead consisted of a blend of reworkable and non-reworkable materials. The non-reworkable ERL has a very similar molecular structure to the α-Terp monomer, but is not reworkable under the rework conditions used because it contains the more thermally stable primary ester bridging group instead of the thermally labile tertiary ester function. Because of their molecular similarities, ERL was expected to mix homogenously with the α-Terp monomer. By combining the two epoxies, a wide range of crosslink densities could be achieved by using a single material set and curing condition. Also, because the α-Terp component was expected to be able to degrade completely, the remaining non-reworkable portions of the network would be expected to have crosslink densities that are directly related to the amount of ERL in the sample. Thus, both the amount of ERL in the system and the rework conditions contribute directly to the extent of the final crosslink densities of the materials.

Table 1 shows the experimental matrix used for the swelling portion of this study. The rework temperature-composition combinations with checkmarks represent

samples that were successfully measured via the swelling experiments. The combinations with × s represent sample treatments that produced materials that did not survive the swelling experiments. The '×' samples completely degraded and/or dissolved in the swelling solvent during the course of the swelling experiment. A cursory explanation for this is that these materials have undergone degradation to such a degree that the remaining network bonds can no longer hold together the network. As would be expected, the longer the rework time and the greater the reworkable content, the greater the chance that the network will completely break apart. A quantitative and more rigorous explanation of this behavior will be provided subsequently.

3.1.2. Glass transition temperature shifts

Fig. 2 shows the T_g-shift results of the samples prior to swelling. Some curves show a continuous decrease in T_g, some show a general increase in T_g and still others show an increase in T_g followed by a decrease. This range of behavior is due to the high-applied rework temperature. At 193 °C, the tertiary ester linkages intrinsic to the α-Terp portions of the network undergo the prescribed degradation. However, the ERL system is known to have an ultimate T_g of between 180 and 190 °C. Thus, a secondary effect of the applied rework conditions is to further cure the ERL portions of the network. The result is that for samples with a high concentration of ERL, T_g first increases on heating because the rate of crosslink formation during the curing process is higher than the rate of crosslink scission via the rework mechanism. As the curing nears completion, the effects of network degradation dominate, and T_g drops. At long rework times, i.e. $t > 150$ min, the T_g stabilizes indicating that both the curing and degradation processes have been completed. These competing effects cannot be avoided, but they do not overly complicate the interpretation of the results.

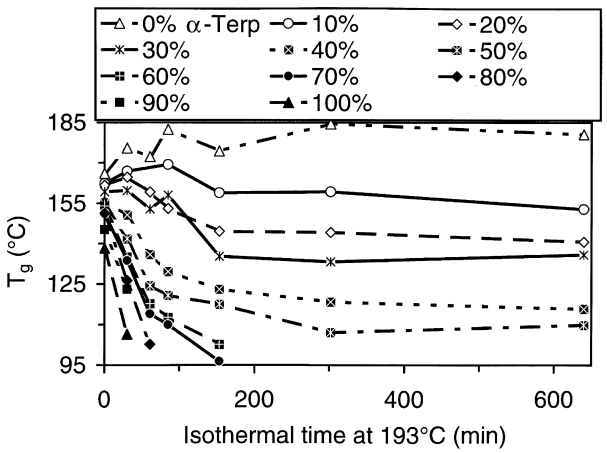

Fig. 2. Glass transition temperatures of the samples used in swelling tests as a function of their rework times. The greater the amount of α-Terp in the material, the lower the T_g.

3.2. Dynamic mechanical thermal analysis

Most of the models developed to calculate strand density were originally intended for use with elastomers, i.e. networks made up of true random coil segments connected at crosslinks [26–28]. Fortunately, the theory of rubber elasticity has been observed to hold for epoxy materials, as long as the measured modulus is below 10 MPa [12]. For most epoxy materials, this issue may be resolved by raising the testing temperature sufficiently above the glass transition temperature of the material. With regard to the particular model chosen, the one representing affine behavior seemed most appropriate. Affine behavior is characterized by network chains and crosslinks that move proportional to the macroscopic deformation of the system. This is in contrast to a phantom network where the crosslinks may fluctuate about their mean positions due to Brownian motion. Due to the low molecular weight between crosslinks, M_C, of our epoxy systems and the small deformations applied during thermal mechanical testing, the affine model should more accurately describe our systems [25].

3.2.1. Strand density versus isothermal time

The results of the isothermal DMTA runs (carried out at 193 °C) expressed in terms of the strand densities, ν_{DMTA}, are shown in Fig. 3. As the isothermal time increases, the changes in strand densities exhibit competing curing and degradation reactions, similar to the T_g-shift results in Fig. 2. Because the DMTA data for each sample is collected continuously throughout the isothermal treatment, there is much less noise associated with the data when compared to the T_g-shift results; however, not all samples could be measured under these conditions. The strand densities of the two samples with ERL concentrations greater than 80% could not be measured at 193 °C due to additional curing of the networks. As more curing took place, their crosslink densities, and subsequently their glass transition

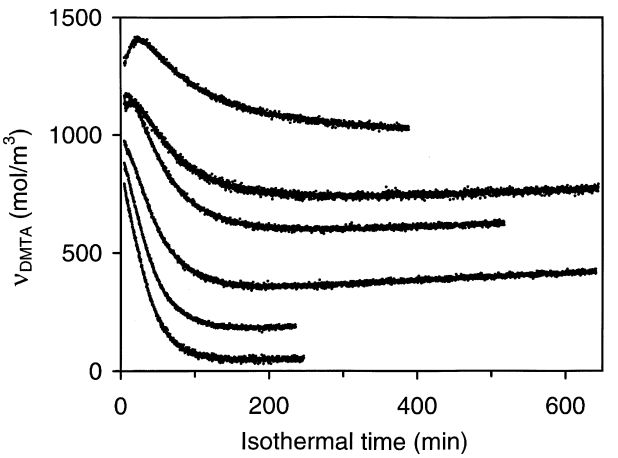

Fig. 3. Strand densities as determined from DMTA measurements. The samples from highest to lowest strand densities are AE19, AE27, AE36, AE46, AE55, and AE66.

temperatures, increased to an extent that the measurements at 193 °C were no longer in the rubbery regime of the samples. In order to obtain crosslink density measurements for AE-0 and AE-10, samples that were previously reworked were tested using a temperature sweep DMTA run at a heating rate of 5 °C/min. The shear modulus at 220 °C was then used to calculate the corresponding crosslink density. Samples that contained more than 70% α-Terp also could not be tested using DMTA methods. At 193 °C, these samples degraded too quickly to permit accurate measurements. After several minutes at these temperatures, the structural integrity of these samples decreased to the point where the samples would physically deform under their own weight, thereby preventing any accurate shear modulus determination.

3.2.2. Strand density versus amount of α-Terp

From Fig. 3, the completion of the degradation reactions is easily identified since the strand density reaches a plateau for each sample, at times greater than 150 min. The strand densities of the completely reworked networks are plotted against the amount of α-Terp in the systems in Fig. 4. A linear regression analysis of the data intersects the zero-strand density axis at approximately 64% α-Terp content. This suggests that reworkable thermoset mixtures with more than 64% reworkable unit can completely lose structural integrity given a sufficient amount of rework. This is consistent with the difficulties encountered during attempts to measure AE-77, AE-88, and AE-100 via DMTA. For an explanation of the significance of this critical content, we turn to percolation theory.

3.3. Percolation theory/DMTA

In general, percolation theory deals with the process of randomly filling in bonds (e.g. chemical bonds) or sites (e.g. crosslinks) on a lattice to form a network [36]. The quantitative results are different depending on which item, bonds or sites, you choose to work with. Because our systems deal with chemical crosslinks, we will discuss everything in terms of site percolation. We will define a *cluster* as any group of sites where each site is connected to at least one of its nearest neighbors. It is automatically assumed that a bond exists between two nearest neighbor sites. Also, we define p as the probability that any given site is occupied. Thus, as p increases, the average size of clusters is expected to increase. When p reaches p_c, the percolation threshold, the largest cluster will span the entire lattice. So for a lattice of infinite span, the percolation threshold represents the transition from having a cluster of finite size to one of infinite size. Due to the complexity of the mathematics, few lattices have exact solutions for the percolation threshold. However, computer simulations and other techniques have yielded accurate values of p_c. For example, a diamond lattice has $p_c = 0.43$, a cubic lattice has $p_c = 0.3116$, and a FCC lattice has $p_c = 0.198$.

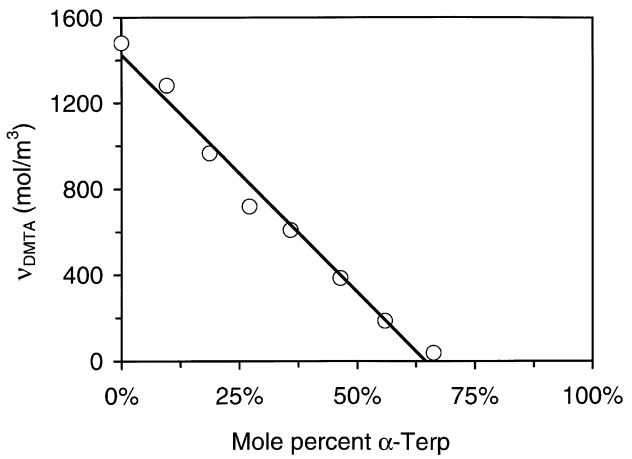

Fig. 4. Strand densities of fully reworked samples as determined from DMTA measurements plotted as a function of their α-Terp concentration. The solid line is intended to guide the eye.

An analogy between our reworkable network and a percolation model exists in the nature of the crosslinked structure, where a reworked ester linkage represents an empty site and a non-reworked site represents an occupied site. An ideal tetrafunctional network may be represented by a diamond lattice such that each junction in the lattice represents a crosslink. Because the α-Terp/ERL system may be assumed to be homogeneously mixed, the distribution of reworkable crosslinks throughout the network should be randomly distributed. Therefore, using a fully reworked sample, i.e. 100% cleavage of tertiary ester linkages, the fraction of non-reworked crosslinks would be equal to the molar fraction of ERL in the system. For a diamond lattice, the site percolation threshold is 0.43. In other words, at least 43% of the epoxy monomer component needs to be ERL in order to maintain a network molecular weight of infinity, even at high degrees of rework. However, the DMTA results indicate that only 36% ERL is necessary to maintain a network of infinite molecular weight. The discrepancy is probably due to the precise nature of the degradation chemistry of the system. Although tertiary ester degradation proceeds to completion, some of the carboxylic acid groups formed react to produce acid anhydride linkage; thus, the resulting decrease in crosslink density is slightly offset by an increase in crosslink density due to anhydride formation. This issue will be examined further in the swelling results section.

3.4. Comparison of DMTA and T_g-shift results

Fig. 5 shows the strand density obtained from DMTA measurements plotted against the corresponding T_g-shift data from Fig. 2. The straight line is a linear fit of the data. There are two important items to note on this particular plot. The first is that the crosslink densities of the reworkable thermosets do vary with their glass transition temperatures. An implication of this observation is that Eq. (4) describes not just the degradation kinetics of the α-Terp network but

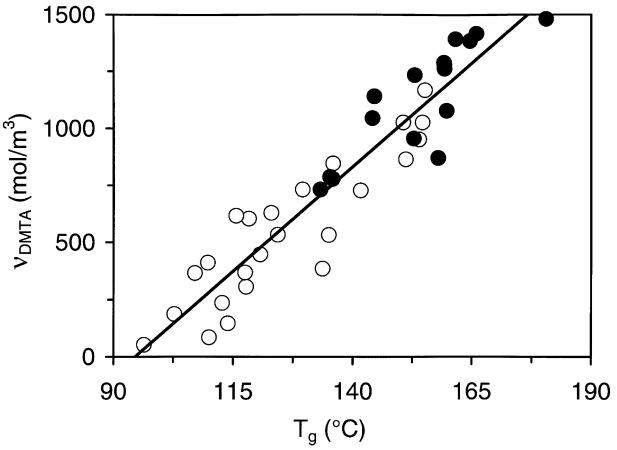

Fig. 5. Strand densities of samples as determined from DMTA measurements plotted as a function of its glass transition temperature. The filled circles represent samples containing more than 70% ERL and the solid line is intended to guide the eye.

also its glass transition temperature behavior. By using Fig. 5 as a calibration curve, Eq. (4) may now be used to predict the crosslink density of a reworkable thermoset given its rework conditions. The second item to note is the point at which a linear regression intersects the zero strand density value, which corresponds to a T_g of 94 °C. Looking back at Table 1 and Fig. 2, the minimum T_g for samples that withstood the entire swelling period is slightly above 95 °C. Therefore, this would seem to indicate that at glass transition temperatures less than 94 °C, networks based on the α-Terp/ERL system would completely lose their structural integrity. Previously published data on the fracture toughness of reworkable thermosets appear to corroborate this [10]. Upon being subjected to a rework thermal cycle, the T_g of those materials went from a maximum of 156–94 °C. This corresponded to a decrease in fracture toughness from 1.76 MPa m$^{1/2}$ to a minimum of 0.20 MPa m$^{1/2}$.

3.5. Swelling

Fig. 6a and b show typical swelling behaviors of the reworkable thermosets. Fig. 6a, which is data for sample AE-46, is representative of materials with high concentrations of α-Terp, whereas Fig. 6b, which presents data for sample AE-10, is representative of materials with high concentrations of ERL. Both AE-46 and AE-10 were annealed for 640 min at 193 °C to fully degrade the network. As the solvent penetrates into the network, samples that undergo little network degradation tend to exhibit the expected swelling behavior where the mass increases linearly with the square root of the swelling time and then tapers off to equilibrium [37]. However, samples that undergo significant network degradation show a much different trend. Initially, the mass increases quickly, but it is then followed by a decrease that slowly levels off. For a few samples, such as AE-46, the decrease in mass continued

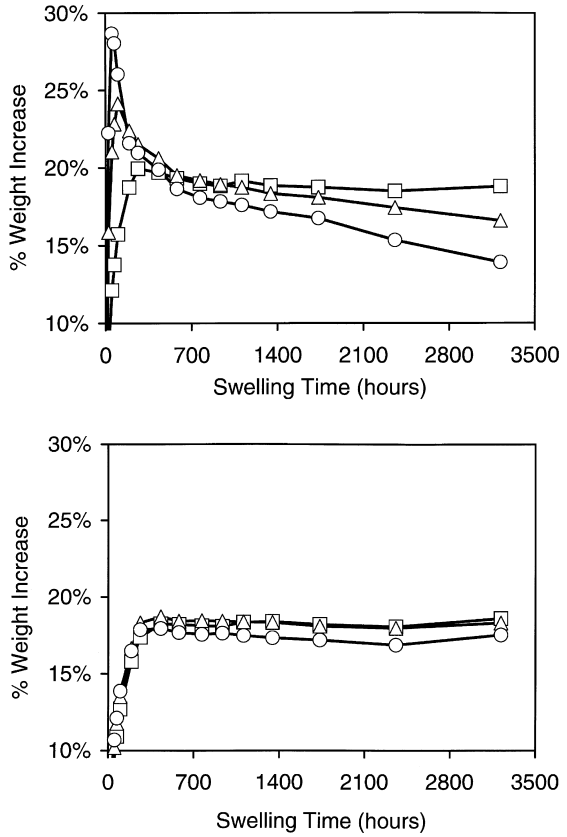

Fig. 6. a (upper) is a representative swelling curve of samples with high α-Terp concentrations, whereas samples with low α-Terp concentrations are represented in b (lower). The data reflects rework times of 0 min (□), 61 min (△), and 640 min (○).

even at the end of the swelling period (19 weeks). However, the decrease in weight changed by less than 0.5% over the course of the final week for all samples, thus justifying an end to the swelling portion of the experiment.

3.5.1. Calculation of χ

In order to use Eq. (2) to calculate the strand density via swelling experiments, the polymer-solvent interaction parameter χ must be known. For the purposes of this paper, χ for the reworkable systems was assumed to be similar to values of χ reported for other anhydride-cured epoxy systems swollen in methanol [38]. The literature value quoted a value of $\chi = 1.05$, however, we chose a calculated value of $\chi = 1.034$. This was done so that a linear regression of $\nu_{swelling}$ versus ν_{DMTA} intercepted the origin, i.e. $\nu_{swelling} = \nu_{DMTA} = 0$. It should be noted that minor changes in the value of χ yielded less than a 5% change in the overall results. A second assumption with regard to χ, made for ease of computation, was that it was constant for all samples. It might be argued that χ would depend on (i) crosslink density or (ii) chemical changes that occur during rework. McKenna and Flynn reported a linear dependence of χ on ν [39]. The effect on our systems would be to shift the calculated values, but have no effect on qualitative trends as ν is already linearly dependent on χ in Eq. (2).

Chemical changes such as the formation of acid groups might lower the value of χ due to increased compatibility with the solvent. However, the excess amount of methanol used during swelling will react quickly with acid groups to form esters, thereby limiting changes to χ. Calculations based on the degree of mass loss and the amount of soluble fraction showed no changes in χ for our systems during the swelling process. In Fig. 7, the difference between the maximum swelling mass and the equilibrium swelling mass was plotted versus the mass of soluble fraction extracted from each sample. The resulting curve with a slope close to unity implies that changes in mass during swelling were due mostly to the soluble portions of the systems and not due to changes in χ.

3.5.2. Strand density versus isothermal time and T_g

Fig. 8 shows the strand densities calculated from swelling experiments plotted against rework time. The data shows the familiar curing and degradation trends seen in the T_g-shift and DMTA experiments. However, unlike the T_g-shift and DMTA results, the larger variations in T_g only become pronounced in samples with higher α-Terp concentrations. This variation is more apparent in Fig. 9 where the T_g-shift data (from Pascault–Williams analysis) is plotted against the respective strand density values [40]. Sample mixtures containing less than 30% α-Terp (more ERL)are highlighted using filled-circles.

There are several possible explanations for these observations. The swelling theories are based on elastomeric networks where the end-to-end distance of the chains between the crosslinks assumed a Gaussian distribution [26–28]. A resulting limitation of the theory is the necessity of having large molecular weights between crosslinks to obtain accurate results. However, this probably is not the primary reason for the observed behavior. The observed difference seems to be associated with samples containing more than 70% ERL and is not very dependent on T_g, which should be a direct indication of strand density. These differences may reside with the subtle variations in chemical

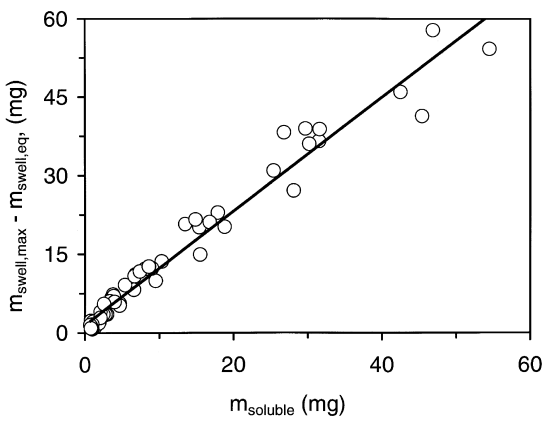

Fig. 7. Differences between the maximum and minimum swelling mass versus the mass of soluble fractions extracted. The solid line represents a linear fit.

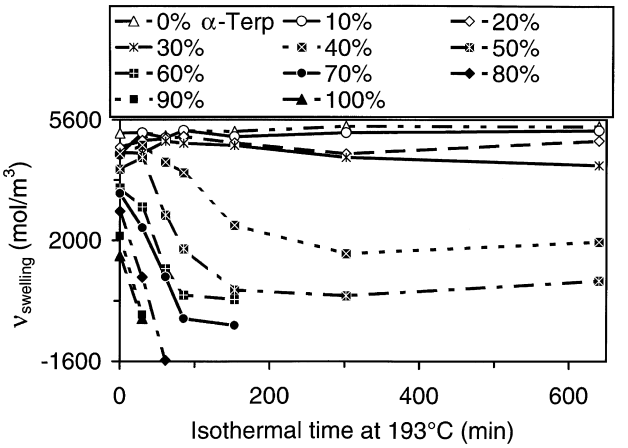

Fig. 8. Strand densities of samples as determined from swelling measurements plotted as a function of their rework time.

structures of the two types of epoxy monomers. In addition to containing a tertiary ester linkage, the α-Terp monomer also contains a methyl-substituent on one of its epoxy groups which may hinder the curing reaction at that site. In contrast, the ERL monomer contains two relatively unhindered epoxy groups. The result is that the ERL system cures more efficiently than the α-Terp system.

Consider again percolation theory. In order to form a continuous string of ERL molecules across the network to the other, it is necessary to have at least 43% ERL in the system. On the other hand, at ERL concentrations greater than 57%, the degraded α-Terp portion will no longer be able to form a continuous structure spanning the entire network. Thus for the samples in question, namely those with ERL concentrations greater than 70%, the swelling equilibrium point may be dominated by an ERL network such that the overall swelling of these samples becomes inhibited. The same effect is not detected in the DMTA experiments because the resulting strains induced in

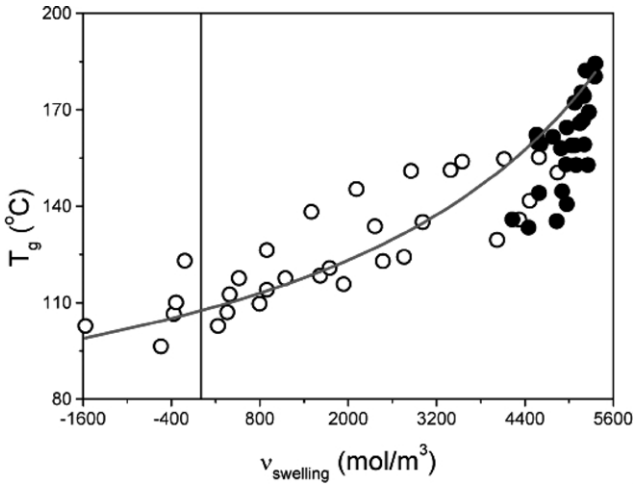

Fig. 9. Strand densities of samples as determined from swelling measurements plotted as a function of their glass transition temperatures. The filled circles represent samples containing more than 70% ERL and the solid line is a Pascault–Williams fit. The vertical line represents $\nu = 0$.

samples are due to externally applied stresses, and not by thermodynamic forces.

Another aspect of the swelling experiments is that some of the samples generated physically unreal negative values of strand density. However, with reworkable thermosets, it is possible to have near-zero crosslink densities. By considering the overall precision of the swelling technique and the known uncertainty in χ, it is not surprising to find some negative values. Despite these uncertainties, the data still offers much useful information. A fit of all the data in Fig. 9 yields a $\nu_{swelling} = 0$ intercept at $T_g = 103$ °C. Even if the samples containing less than 30% α-Terp are discounted, the intercept remains about the same. This intercept was expected to be similar to the value obtained via DMTA calculations because of the way in which χ was optimized. In Fig. 10, $\nu_{swelling}$ of samples that were reworked for 640 min was plotted versus the α-Terp concentration of the samples. Inspection of the plot yields a zero crosslink density intercept of ~50% α-Terp. Again, if the samples containing less than 30% α-Terp are discounted and χ is adjusted accordingly, the intercept shifts to 54%. This is much closer to the 57% α-Terp/43% ERL intercept expected from percolation theory when compared to the DMTA results, but this does raise the issue of why there exists such a significant shift from the DMTA determined intercept of 64% α-Terp concentration. The answer may lie in the degradation chemistry of the system. As mentioned in the DMTA analysis section, some of the degraded components react at high temperatures to form acid anhydride crosslinks. However, methanol is known to readily break anhydride bonds to form carboxylic acids and esters. The result is that after swelling, only the ERL portions of a fully reworked sample will contribute crosslinks to the network. In contrast, there is no mechanism in the solid state to eliminate the anhydride links.

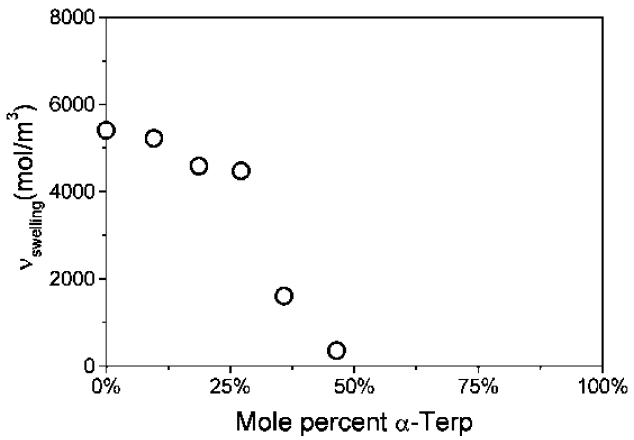

Fig. 10. Strand densities of fully reworked samples as determined from swelling measurements plotted as a function of the α-Terp concentration.

3.6. Comparison of DMTA and swelling results

In Fig. 11, the strand densities as calculated by swelling are compared to that obtained via DMTA. The linear relationship helps add confidence to the results and interpretations obtained by swelling. However, there is a factor of 4.4 difference between the quantitative results, with the swelling results yielding much higher crosslink density values than DMTA. The results of Murayama and Bell showed a similar trend for an amine-cured epoxy system [14,15]. On average, the M_C values they had calculated via swelling and via mechanical measurements differed by a factor of 3.5. However, they did not provide an explanation for their observations. We believe the discrepancies are due in part to the limitations of the Flory–Rehner equation. As mentioned earlier, the Flory–Rehner expression was derived assuming that the end-to-end distance of the chains between the crosslinks took on a Gaussian distribution. The molecular weight between crosslinks for the reworkable epoxy systems has a lower limit of only a few hundred grams per mole, thus nullifying Flory and Rehner's assumption. Application of this theory to our thermosets assumes the networks could swell more than they actually did, which in turn would result in an overestimation of the strand densities. The effects of this should be more evident in samples with higher concentrations of ERL as these particular samples would have lower M_Cs. In samples with high concentrations of α-Terp, degraded components may behave as plasticizers in the network, thereby reducing the modulus and T_g of the materials. This should have no effect on the swelling results because the small molecules are extracted during the swelling process; however, the effect on DMTA samples would be an underestimation of the strand density.

3.7. Gel degradation theory and Macosko–Miller branching theory

Several industrial processes also involve the decomposition of polymer networks. The degradation mechanism of

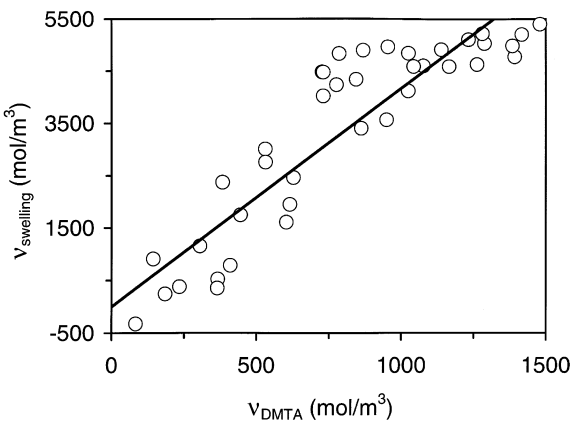

Fig. 11. Comparison of strand densities calculated from swelling and DMTA measurements. The solid line represents a linear fit.

our reworkable thermosets may be conceptually comparable to the delignification of wood [41–44]. A major component of wood is lignin, a complex organic molecular network. During the chemical pulping process of wood, the lignin network is broken down in a process known as delignification where crosslinks are broken chemically. Szabo and Goring postulated that the process could be modeled by applying the Flory–Stockmayer theory of trifunctional polymerization in reverse [42]. Several groups working with model trifunctional networks have found strong evidence supporting the idea that random network degradation is the reverse of network formation [18–20,45]. Although our systems are tetrafunctional, the same ideas concerning gel degradation should hold true for reworkable thermosets.

In Fig. 12a, the soluble materials extracted from the swelled samples were plotted as a percentage of the sample's original weight versus the α-Terp concentration. As expected, samples containing more α-Terp and reworked for longer periods of time exhibited the greatest weight percent of soluble materials. It is interesting to note that the data points for rework times greater than 153 min all seem to lie on a single curve. This is to be expected because the network degradations were nearly complete at isothermal times longer than 150 min. To better evaluate this information, the weight percent of soluble fractions was re-plotted against the amount of network degradation in Fig. 12b. The degree of network degradation is inferred from the glass transition temperature of the material and was calculated from data in Figs. 9 and 10, the details of which may be found in Appendix A. In Fig.12b, the data of Fig. 12a now collapses onto a single curve. If the rework process is in fact analogous to a reversal of the gelation process, then the data should be representative of the weight fraction of soluble fractions during the crosslinking of a tetrafunctional network. Using a conditional probability approach, Macosko and Miller developed a set of expressions relating the post-gel properties of a variety of network polymers to the extents of reaction [21,22,25,46]. These expressions were used to calculate the weight fraction of soluble fractions versus the extent of curing reaction for the reworkable materials. Even though our material cures like an $(A_4 + B_2)$ system, the degradation mechanics of our system most resembles that of a tetrafunctional homopolymer polymerization in reverse. Given that, the expression employed for a tetrafunctional homopolymer is given as

$$w_s = P(F_A^{out})^4 \tag{5}$$

where w_S is the weight fraction of soluble fractions, and $P(F_A^{out})$ is the probability that looking 'out' from a functional group leads to a finite chain [46]. This is given by

$$P(F_A^{out}) = \left(\frac{1}{p} - \frac{3}{4}\right)^{\frac{1}{2}} - \frac{1}{2} \tag{6}$$

where p is the extent of reaction. Assuming the gel degradation theory holds, the weight fraction of soluble fractions as a function of the extent of degradation should be equal to the weight fraction of soluble fractions as a function of $(1 - p)$, i.e. one minus the extent of curing reaction. In Fig. 12b, the weight fraction of soluble fractions calculated using Macosko and Miller's expressions is plotted against (1 − extent of degradation). The excellent fit provides strong evidence that gel degradation theory is able to well-describe the behavior of the present reworkable thermosets. To take this one step further, Macosko and Miller's expressions for calculating the strand density were used and the results were compared to those obtained via DMTA. The expression for finding the strand density of a tetrafunctional system is given by

$$\nu = \frac{\rho}{M_n}([1 - P(F_A^{out})]^4 + 4P(F_A^{out})[1 - P(F_A^{out})]^3) \tag{7}$$

where ρ is the density of the system and M_n is the molecular weight between crosslinks. For our calculations, the average density of all samples was used, and M_n was taken to be the average epoxy monomer molecular weight plus the molecular weight of two anhydride hardening units. There is very good correlation between the calculated Macosko–Miller values and the experimental values, adding credence to the applicability of the gel degradation theory (Fig. 13).

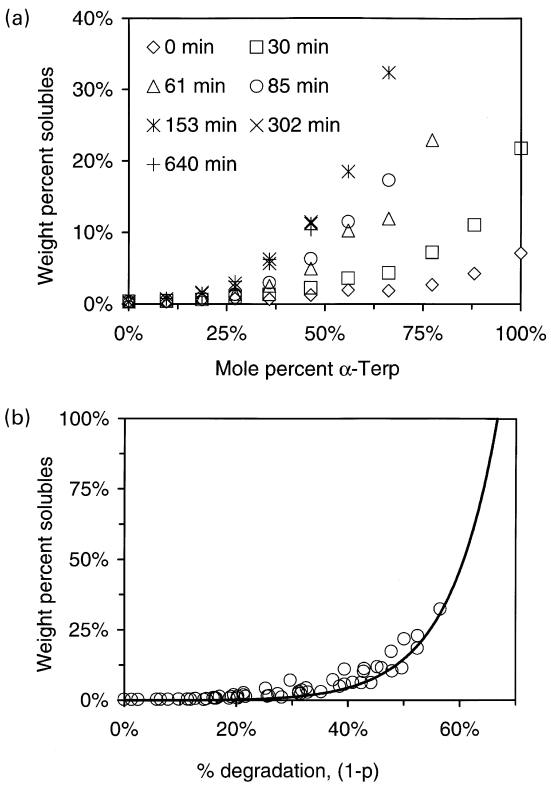

Fig. 12. a (upper) shows the weight percent of soluble materials as a function of the α-Terp concentration. The same information is plotted against the extent of degradation in b (lower). The solid line in b was calculated using Macosko and Miller's branching theory [21,22].

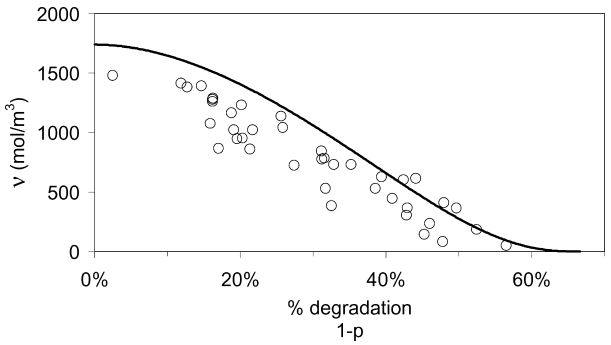

Fig. 13. Strand densities (open circles) as calculated from DMTA measurements compared to values calculated using Macosko and Miller's branching theory (line) [21,22].

4. Conclusions

The role of the time and temperature dependent crosslink density of reworkable thermosets and its effect on physical properties was assessed via glass transition temperature measurements, thermal-mechanical measurements, and solvent swelling measurements. All yielded qualitatively similar results. The strand densities calculated from DMTA measurements were lower than those calculated by swelling measurements. This difference is likely due to limitations in the Flory–Rehner expressions as well as the possibility of the reworked (degraded) components behaving as plasticizers in these networks.

Comparisons of the quantitative results revealed several interesting aspects about the reworkable nature of these materials. The extrapolated zero-crosslink density values showed that reworkable materials containing up to roughly 36 mol% non-reworkable components could be completely degraded, i.e. achieve zero crosslink density, by simply heating the samples at the rework conditions. Nearly all of the tertiary ester linkages were cleaved under these thermal conditions, but the high temperatures caused some of the degraded components to form new anhydride crosslinks. Fortunately, the anhydride crosslinks could be eliminated with the use of appropriate solvents (as carried out in swelling studies), thus enabling reworkable materials containing up to roughly 45 mol% non-reworkable components to be completely degraded. This result correlates well with the percolation threshold of a diamond lattice.

The relationships between the strand density calculations and the T_g-shift results were used to convert the glass transition temperatures of the samples into absolute percent degradation values. This allowed comparison of the experimental results with calculated values using Macosko and Miller's branching theory [21,22]. These results also demonstrated that our reworkable thermosets degrade in a manner consistent with gel degradation theory.

Acknowledgements

Funding from the Semiconductor Research Corporation and IBM Corporation for a fellowship for JC are gratefully acknowledged. Many thanks are due to L. Crane, A. Torres-Filho, P. Klemarczyk, and Loctite Corporation for their support and supply of the α-Terp resin. Thanks to K. Papathomas and G. Kohut at IBM for their useful discussions. Thanks are also due to S. Yang, Y.C. Bae, H. Koerner, and the Ober research group for their advice and support.

Appendix A. Conversion of T_g to percent degradation

It is assumed that in Fig. 10, the mole percent α-Terp of a completely reworked material is equivalent to the percent degradation of the overall network. For example, consider a sample containing 20% α-Terp. Once the sample is completely reworked, contributions to the network will only come from the ERL portion which constitutes 80% of the original network. In other words, 20% of the network has degraded.

To convert a sample's glass transition temperature to a percent degradation value, glass transition temperatures of samples as a function of their strand densities as determined from swelling measurements (Fig. 9) were fit to a Pascault–Williams equation* [40].

$$\frac{T_g - T_{g,min}}{T_{g,max} - T_{g,min}} = \frac{\lambda x}{1 - (1 - \lambda)x} \tag{A1}$$

where

$$x = \frac{\nu_{swelling}}{\nu_{swelling,max}}$$

corresponds to the percent degradation calculated from our swelling experiments. $T_{g,max} \approx 182.2$ °C and $\nu_{swelling,max} \approx 5373$ mol/m^3 are the glass transition temperature and the strand density, respectively, of a 100% ERL material with 0% degradation (derived from Figs. 2 and 8). $T_{g,min}$ represents the glass transition temperature of a completely reworked 100% α-Terp material. Both $T_{g,min}$ and λ serve as fitting variables to obtain an optimal fit of the experimental data with the equation above (Fig. 9). Once $T_{g,min}$ and λ have been determined, an expression can be derived to relate any T_g to a percent degradation as the following.

$$\%\text{Degradation} = x = \left(1 + \frac{T_{g,max} - T_g}{T_g - T_{g,min}}\lambda\right)^{-1} \times 100\% \tag{A2}$$

References

[1] Encyclopaedia Britannica Online, http://search.eb.com/bol/topic?eu = 129061&sctn = 2.

[2] May CA. Epoxy resins: chemistry and technology, 2nd ed. New York: Marcel Dekker; 1988.
[3] Seraphim DP, Lasky R, Li C-Y. Principles of electronic packaging. New York: McGraw-Hill; 1989.
[4] Gilleo K, Blumel D. Int Symp Microelectron 1998;1999.
[5] Buchwalter SL, Kosbar LLJ. Polym Sci, Polym Chem 1990;34: 249–60.
[6] Afzali-Ardakani A, Buchwalter SL, Gelorme JD, Kosbar LL, Newman BH, Pompeo FL. US Patent 5 512 613, 1996 (assigned to IBM Corp.).
[7] Yang S, Chen JS, Korner H, Breiner T, Ober CK, Poliks MD. Chem Mater 1998;10:1475–82.
[8] Stephanie J, Kuczynski J. Proc Tech Prog NEPCON West'97 Conf 1997;364–79.
[9] Wang LJ, Wong CP. J Polym Sci, Polym Chem 1999;37:2991–3001.
[10] Chen JS, Ober CK, Poliks MD. Polymer 2002;43(1):131–9.
[11] Glad MD. Cornell University PhD Thesis; 1986.
[12] Nielsen LE. J Macromol Sci—Rev Macromol Chem 1969;C3:69.
[13] Lemay JD, Swetlin BJ, Kelley FN. Acs Symp Ser 1984;243(165):183.
[14] Bell JP. J Polym Sci, Part a-2-Polym Phys 1970;8:417.
[15] Murayama T, Bell JP. J Polym Sci, Part a-2-Polym Phys 1970;8:437.
[16] Hale A, Macosko CW, Bair HE. Macromolecules 1991;24:2610–21.
[17] Dimarzio EA. J Res Nat Bureau Standards Sec a—Phys Chem 1964; A68:611.
[18] Argyropoulos DS, Bolker HI. Macromolecules 1987;20:2915–22.
[19] Argyropoulos DS, Bolker HI. Makromolekulare Chemie-Macromol Chem Phys 1988;189:607–18.
[20] Argyropoulos DS, Bolker HI. J Wood Chem Technol 1987;7: 499–511.
[21] Miller DR, Macosko CW. Macromolecules 1976;9:206–11.
[22] Macosko CW, Miller DR. Macromolecules 1976;9:199–206.
[23] Flory PJ. Polymer 1979;20:1317–20.
[24] Kuhn W. Kolloid Zeits 1936;76:258.
[25] Queslel JP, Mark JE. Adv Polym Sci 1984;65:135–76.
[26] Flory PJ. Principles of polymer chemistry. Ithaca: Cornell University Press; 1953.
[27] Flory PJ, Rehner Jr J. J Chem Phys 1943;11:521–6.
[28] Flory PJ, Rehner Jr J. J Chem Phys 1943;11:512–20.
[29] Patel SK. Cornell University PhD Thesis; 1991.
[30] Banks L, Ellis B. Polymer 1982;23:1466–72.
[31] Bellenger V, Verdu J, Morel E. J Mater Sci 1989;24:63–8.
[32] Bellenger V, Verdu J, Morel E. J Polym Sci, Part B—Polym Phys 1987;25:1219–34.
[33] Gonis J, Simon GP, Cook WD. J Appl Polym Sci 1999;72:1479–88.
[34] Gupta VB, Drzal LT, Lee CYC, Rich M. J Polym Engng Sci 1985;25: 812–23.
[35] Patel SK, Malone S, Cohen C, Gillmor JR, Colby RH. Macromolecules 1992;25:5241–51.
[36] Stauffer D, Amnon A. Introduction to percolation theory, 2nd ed. London: Taylor and Francis; 1992.
[37] Rossi G, Mazich KA. Phys Rev E 1993;48:1182–91.
[38] Jackson PL, Huglin MB, Cervenka A. Polym Int 1994;35:135–43.
[39] McKenna GB, Flynn KM, Chen YH. Polymer 1990;31:1937–45.
[40] Venditti RA, Gillham JK. J Appl Polym Sci 1997;64:3–14.
[41] Bolker HI, Brenner HS. Science 1970;170:173.
[42] Szabo A, Goring DAI. Tappi 1968;51:440.
[43] Yan JF. Macromolecules 1981;14:1438–45.
[44] Leclerc DF, Olson JA. Macromolecules 1992;25:1667–75.
[45] Yan JF, Johnson DC. J Appl Polym Sci 1981;26:1623–35.
[46] Valles EM, Macosko CW. Macromolecules 1979;12:673–9.